9-13-2002

Density and Conformation with Relaxed Substrate, Bulk, and Interface in Electrophoretic Deposition of Polymer Chains

F.W. Bentrem
University of Southern Mississippi

J. Xie
University of Southern Mississippi

Ras B. Pandey
University of Southern Mississippi, ras.pandey@usm.edu

Density and conformation with relaxed substrate, bulk, and interface in electrophoretic deposition of polymer chains

Frank W. Bentrem, Jun Xie, and R. B. Pandey

Department of Physics and Astronomy, The University of Southern Mississippi, Hattiesburg, MS 39406-5046

Abstract

Characteristics of relaxed density profile and conformation of polymer chains are studied by a Monte Carlo simulation on a discrete lattice in three dimensions using different segmental (kink-jump K, crank-shaft C, reptation R) dynamics. Three distinct density regimes, substrate, bulk, and interface, are identified. With the KC segmental dynamics we find that the substrate coverage grows with a power-law, $d_s \propto t^{\gamma}$ with a field dependent nonuniversal exponent $\gamma = 0.23 + 0.7E$. The bulk volume fraction d_b and the substrate polymer density (d_s) increases exponentially with the field ($d_b \propto E^{0.4}$, $d_s \propto E^{0.2}$) in the low field regime. The interface polymer density d_f increases with the molecular weight. With the KCR segmental dynamics, bulk and substrate density decreases linearly with the temperature at high temperatures. The bulk volume fraction is found to decay with the molecular weight, $d_b \propto L_c^{-0.11}$. The radius of gyration remains Gaussian in all density regions.

Key words:
Polymer, Deposition, Monte Carlo

1 Introduction

One of the common processes to design polymeric materials (including composites) and to coat surfaces [1,2] is to deposit polymer constituents on a desirable substrate and equilibrate. A driving (biased) field caused by electric field, pressure gradient, gravitation, spinning processes, etc., is generally used to direct the deposition and control the morphological evolution. In DNA gel electrophoresis for example, the chain macromolecules are driven by an electric field [3,4]. The flow of DNA molecules through pores and their accumulation at the pore boundaries along the flow direction depend on the magnitude of

the flow field, molecular weight, and porosity (i.e., the size of the pores), etc. As the polymer chains deposit on an impenetrable substrate, the polymer density grows and an interface develops [5,6,7,8]. The interface width defined by the longitudinal fluctuation in density profile is a measure of the roughness of the growing surface [9,10]. Enormous efforts have been devoted to understanding the conformation and density profiles at/near the surface; the list of references is too large to cite them all, but we provide here a few examples [11,12,13,14,15,16] without any preference. However, studies of the interface growth, conformation and density profile for the electrophoretic deposition of polymer chains on the impenetrable substrate [5,6,7,8] are very limited. The characteristics of the density profile, growth of the interface width, and roughness depend on the deposition process, parameters such as driving field, temperature, and molecular weight, and the relaxation procedures.

Since the polymer chains, driven by a field, deposit on an impenetrable substrate/wall, their conformational phase space at the substrate is constrained. The polymer density grows from the substrate as the deposition proceeds which leads to evolution of the bulk region adjacent to the substrate. Distinct regimes emerge from initiating growth at the substrate toward the source at the opposite end from where the polymer chains are released: substrate, bulk, interface, and dilute solution. Movement of chain segments, their relaxation, and degree of entanglement may vary from one regime to another. Parameters such as temperature, molecular weight, field, and procedure such as segmental dynamics and relaxation may also affect the characteristics of these regimes. Therefore, it would be interesting to study how the polymer density varies from one region to the next and how it depends on these parameters.

While it is difficult to monitor and control deposition process, density profile, polymer conformation, etc. at the molecular scales in the laboratory, computer simulation experiments can be implemented to examine these properties with simplified models [17]. Making quantitative predictions by analytical theories is severely limited in such a complex system involving different phases of material, interfaces, and relaxation at various scales. Therefore, computer simulation experiments may be useful to gain insight into some of the difficult issues such as prediction of density profile and its dependence on molecular weight, field and temperature. In recent articles, we have reported our analysis of the interface growth and its scaling [6,7,8,18]. Using the same computer simulation model on a discrete lattice we would like to study characteristics of the density profile and conformation of chains in this paper. Model is presented in the next section followed by results and discussion in section 3 with a conclusion at the end.

2 Model and Method

We consider a discrete lattice of size $L_x \times L \times L$ with a large aspect ratio L_x/L. Coarse-grained polymer chains, each of length L_c (i.e., $(L_c + 1)$ nodes connected by bonds) are generated on trails of random walks along the lattice with excluded volume constraints toward the source end ($x = 1$). An external field E drives the chains toward the substrate (impenetrable wall) at $x = L_x$. The change in energy due to the field

$$\Delta U = E \cdot \Delta x, \tag{1}$$

where Δx is the displacement of the chain node along x direction. We also consider a nearest-neighbor polymer-polymer repulsive and polymer-wall attractive interaction,

$$U = J \sum_{ij} \rho_i \rho_j, \tag{2}$$

where $J = 1, \rho_i = 1$ if the site i is occupied by the polymer node, 0 if the site i is empty, and -1 if the empty site i is on the substrate. The summation is restricted to nearest neighbor sites. Chains are released at a constant rate (typically one every hundred time steps) and moved with the Metropolis algorithm [19] using a combination of segmental movements [17], i.e., kink-jump, crankshaft [20], and slithering snake (reptation) dynamics. Attempt to move each chain node once is defined as one Monte Carlo step (MCS). The simulation is performed for a relatively large number of time steps for a sufficiently large number of independent samples to obtain a reliable estimate of the averaged physical quantities.

Polymer chains move from the source end toward the impenetrable substrate at the opposite end by the field (E) using different segmental dynamics. Kink jump dynamics involves movement of only one node and it is relatively slow and localized. Therefore, it takes much longer to relax the polymer chains. Crank-shaft involves movements of two nodes simultaneously, and it is faster than kink-jump but still localized to small part of chain's segment. Slithering-snake ("reptation") dynamics, on the other hand, involves global motion of the whole chain by altering conformations at the end segments. Perhaps, a combination of these and other modes of segmental movements are desirable in many polymer simulations. We will, however, concentrate here with combinations of three segmental dynamics, (i) kink-jump (K), (ii) kink-jump and crank-shaft (KC), and (iii) kink-jump, crank-shaft, and reptation (KCR). Apart from the segmental dynamics, a relaxation procedure [18]is also implemented to equilibrate the polymer conformation and density. If we continue to deposit polymer chains and monitor the evolution of the density and conformational profiles, interface width, etc., we reach a steady-state where these quantities approach their steady-state (constant) value in asymptotic time steps [6,7,8]. However, if we stop releasing new chains after an appropriate, i.e., desirable

growth while allowing chains to execute their segmental moves, we find [18] a considerable change in the interface width (i.e., the roughness). We have recently reported [18] scaling behaviors of the "relaxed" interface width and pointed out the differences from their "steady-state" values. In this paper, we present our results of relaxed data for the density profile and conformation.

3 Result and Discussion

Most of our simulations are performed on a $100 \times 40 \times 40$ lattice with the size of polymer chains $L_c = 10 - 100$ at various temperatures and fields. A number of independent samples $N_s = 10 - 20$ are used to average the physical quantities. Different lattice sizes are also used to check for the severe finite size effect and no significant difference is observed in the qualitative behavior of the physical quantities reported here. We have already reported the growth and scaling of the interface width including roughness in a series of papers in recent years [6,7,8,18] by analyzing steady-state and relaxed interface width. In this article we concentrate on the characteristics of the density in various regimes. Our data on the conformation of chains in these regimes have relatively large fluctuations and therefore, their qualitative analysis will be limited.

Some studies for polymer melts near an impenetrable wall [5,11,12,16] have indicated an oscillation in the density profile near the wall. Other studies have shown a parabolic [21,22] or hyperbolic [23] decay in density with distance from the wall. For our simulations relaxed density profiles with K, KC, and KCR dynamics are presented in Figs. 1-3, respectively, at the temperature $T = 1$ for different driving fields. Even though the chain lengths are different ($L_c = 39, 39, 50$), the qualitative forms of their density profiles should be comparable for the following reason. We have examined the relaxed density profiles with different chain lengths $L_c = 10 - 100$ and have found no significant difference in their density profile (independent of chain length) for any combination of the segmental dynamics we have studied here. A careful examination of these profiles (Figs. 1-3), however, reveals some differences due to segmental dynamics. Figure 4 shows an example for such a comparison at $T = 1, E = 0.2$ with K, KC, and KCR segmental dynamics. We see that the polymer density in most regions (particularly at the substrate and in the bulk) is highest with the KCR dynamics and lowest with the K dynamics as it is slowest in relaxing the chains and is restricted to very short range local moves. Reptation (slithering-snake) movements in KCR dynamics involves long range fast movements which helps equilibrating the polymer density better than the short-range moves with K and KC segmental dynamics.

Obviously, there is a profound effect of the field in orchestrating the shapes of the density profiles. A more specific examination will follow later. It is worth

pointing out that we have not observed any sign of oscillations in density profiles as observed with the steady-state density profiles with a combination of kink-jump and reptation dynamics [6]. Further, there is clogging with the kink-jump segmental dynamics alone particularly at higher values of field ($E \leq 0.6$, see Fig. 1). With clogging, the rate of polymer deposition on the substrate is hard to monitor and different from that without clogging. Such a problem with the K segmental dynamics is also reported in study of the interface growth and its scaling. In the following we restrict most of our analysis to KC and KCR dynamics where the clogging is not a problem for the range of parameters we have explored here. Thus, mixing different segmental movements along with relaxation (without additional deposition) is important in relaxing the polymer chains, avoiding the clogging, equilibrating the density distribution, and reducing the probability of layering in density profile of driven polymer deposition.

Figure 5 shows the density profiles at different temperatures with KC and KCR segmental dynamics at a fixed field $E = 0.5$. Again we see the differences due to segmental dynamics along with the effect of temperature, which is revisited later.

Let us examine the characteristics of density in each region, i.e., substrate ($x = L_x$), bulk (between substrate and the interface), interface, and dilute solution (fluid), of the density profile. Polymer density in bulk is referred to as the volume fraction and density at the substrate as the coverage, the fraction of sites covered by the polymer. Figure 6 shows the growth of coverage with KC segmental dynamics. Note that the coverage, d_s, grows rather fast initially followed by a slow growth before reaching its saturation, the asymptotic value also known as jamming coverage. It is worth pointing out that the approach to jamming coverage for objects of different shapes and sizes has been notoriously slow and extensively studied [24,25,26,27,28,29,30,31]. While the substrate coverage in steady-state polymer deposition shares the slow approach to the asymptotic (jamming) limit, equilibration by relaxing chains enhances the probability of approaching the jamming limit substantially. In the pre-asymptotic regime, growth of the coverage seems to grow with a power law (see Fig. 7),

$$d_s \propto t^{\gamma}, \tag{3}$$

with an exponent γ. The coverage growth exponent γ is found to depend on the field (see Fig. 8),

$$\gamma = 0.23 + 0.7E, \tag{4}$$

and is therefore, non-universal.

Relaxed densities in the bulk, i.e., the volume fraction d_b and the substrate coverage d_s depend on the field in low field regime ($E \leq 0.5$) as seen in Fig. 9. The volume fraction and the coverage increase with the field exponentially and become constant at their maximum values at high fields. The polymer

density at the interface d_f, on the other hand, is found to increase with the field with a power law (see Fig 10). Best fits of our data suggest,

$$d_f \propto E^{0.3},\ d_b \propto E^{0.4},\ d_s \propto E^{0.2}. \tag{5}$$

The response of polymer density to field in the low field regime seems to be stronger with the relaxed system here than the corresponding response with a steady-state simulation.

The interface polymer density also seems to increase with the molecular weight. Best fit of our data in Fig. 11 leads to,

$$d_f = 0.4 + 0.0002 L_c \tag{6}$$

It is worth mentioning that a similar trend for the dependence of volume fraction and coverage on the field is also observed with the kink-jump dynamics except the range of field for the growth of density is reduced.

We have also analyzed the temperature dependence of polymer densities in these regions (substrate, bulk, interface). Generally, the density decreases with the temperature. The substrate coverage and the bulk volume fraction show a larger rate of decay than the polymer density at the interface. Volume fraction in bulk shows the largest variation with the temperature for the KCR segmental dynamics as shown in Fig. 12. Best fits of our data in high temperature regime show,

$$d_b = 1.02 - 0.015T,\ d_s = 1.00 - 0.0013T \tag{7}$$

Since the conformation of polymer chains at the substrate and in the bulk are more restricted due to the presence of neighboring chains and their entanglement, increasing the temperature further reduces the conformational entropy. Thus we are able to characterize the dependence of volume fraction and substrate coverage on field, temperature and the molecular weight.

The bulk density is found to decay with the molecular weight as shown in Fig. 13,

$$d_b \propto L_c^{-0.011} \tag{8}$$

Note that the decay of bulk density with the molecular weight shows a similar pattern with steady state simulation with KCR segmental dynamics. Exponential decay is observed with a steady-state simulation involving reptation and kink-jump. We know that it is difficult to pack many chains in a limited volume due to steric hindrance. The larger the chain length the fewer the chains are needed to reach the jamming limit. The percolation threshold [32] of chains and its jamming volume fraction have been found [30] to decay with the chain length in the percolation of chains. Our result seems consistent with the percolation of chains.

We have also analyzed the conformation of polymer chains. In general, our

data for the conformational profiles are more fluctuating than corresponding density profiles. Therefore, at present, we are unable to draw more meaningful conclusion that what is presented here. Figure 14 shows the variation of the radius of gyration of chains at the interface, substrate, and in the bulk, with the chain length on a log-log scale. We see that the transverse component of R_g scales with the molecular weight with,

$$R_{gt} \propto L_c^{\nu_t},\ \nu_t \sim 0.6 \tag{9}.$$

The total radius of gyration shows a Gaussian scaling,

$$R_g \propto L_c^{1/2}. \tag{10}$$

The longitudinal component saturates at higher molecular weight as chains compress.

4 Conclusion

Electrophoretic deposition of polymer chains on an impenetrable substrate is examined by a computer simulation model on a discrete lattice. A combination of different segmental dynamics is used to relax the polymer chains and monitor the density profile. We find that the relaxation of polymer chains, density, and the interface width depend on the segmental dynamics, molecular weight, field, and temperature. The combination of slow-to-fast segmental dynamics is highly desirable to equilibrate our system effectively in our observation time.

Different spatial regions of the material evolved from the polymer deposition, substrate, bulk, and the interface are identified and their physical properties are analyzed. We are able to make a number of quantitative predictions regarding the dependence of relaxed density and conformation of chains in these regions based on our data. We have found that there is very little (negligible) effect of molecular weight on the the relaxed density profiles both with KC and KCR segmental dynamics. With the KC segmental dynamics, we find that the substrate coverage in the pre-saturation regime grows with a power law with a nonuniversal exponent γ (Eqs. 3 and 4). Bulk volume fraction (d_b) and the jamming substrate coverage grow exponentially with the field (Eq. 5). The interface polymer density (d_f) increases linearly with the molecular weight (Eq. 6).

With the KCR dynamics, we are able to attain better defined distinct density regions with relatively less fluctuations. Both bulk volume fraction and substrate coverage are found to decay linearly with the temperature in the high-temperature regime. The bulk density decays with the molecular weight with a power law exponent 0.11 (Eq. 8).

The radius of gyration exhibits a Gaussian conformation in almost all regions. While the transverse component of the radius of gyration scales with an exponent (0.6) similar to that of a self-avoiding walk, the longitudinal components seem to saturates with higher molecular weight. Further large scale simulations are needed to clarify the conformational profile.

Acknowledgments: We acknowledge partial support from a DOE-EPSCoR grant.

References

[1] G. E. F. Brewer (ed.), *Electrodeposition of Coatings* (ACS, Washington, 1973).

[2] R. P. Wool, *Polymer Interfaces: Structure and Strength* (Hanser Publishers, New York, 1995).

[3] O.J. Lumpkin, P. Djardin, and B.H. Zimm, Biopolymers, **24** 1573 (1985).

[4] S.R. Quake, H. Babcock, and S. Chu, Nature, **388**, 151 (1997); T.T. Perkins, D.E. Smith, and S. Chu, Science, **276**, 2016 (1997).

[5] G. M. Foo and R. B. Pandey, Phys. Rev. Lett., **80**, 3767 (1998).

[6] G. M. Foo and R. B. Pandey, Phys. Rev. E, **61**, 1793 (2000).

[7] G.M. Foo and R.B. Pandey, Biomacromolecules, **1**, 407 (2001).

[8] F. W. Bentrem, R. B. Pandey, and F. Family, Phys. Rev. E, **62**, 914 (2000).

[9] A.-L. Barabasi and H. E. Stanley, *Fractal Concepts in Surface Growth* (Cambridge University Press, Cambridge, 1995).

[10] F. Family and T. Vicsek (eds.) *Dynamics of Fractal Surfaces* (World Scientific, Singapore, 1991).

[11] J.-S. Wang and K. Binder, J. Phys. I France, **1**, 1583 (1991).

[12] S. Sen, J. D. McCoy, S. K. Nath, J. P. Donley, and J. G. Curro, J. Chem. Phys., **102**, 3431 (1995).

[13] W. C. Forsman and B. E. Latshaw, Poly. Eng. Sci., **36**, 1114 (1996).

[14] A. V. Dobrynin, Phys. Rev. E, **63**, 51802 (2001).

[15] G. W. Collins, S. A. Letts, E. M. Fearon, R. L. McEachern, and T. P. Bernat, Phys. Rev. Lett., **73**, 708 (1994).

[16] R.B. Pandey, A. Milchev, and K. Binder, Macromolecules, **30**, 1194 (1997), and references therein.

[17] K. Binder (ed.), *Monte Carlo and Molecular Dynamics Simulations in Polymer Science* (Oxford University Press, New York, 1995).

[18] F. W. Bentrem, J. Xie, and R. B. Pandey, Phys. Rev. E, Submitted.

[19] N. A. W. Metropolis, A. W. Rosenbluth, M. N. Rosenbluth, A. H. Teller, and E. Teller, J. Chem. Phys., **21**, 1087 (1953).

[20] P. H. Verdier and W. T. Stockmayer, J. Chem. Phys., **36**, 227 (1962).

[21] S. T. Milner, T. A. Witten, and M. E. Cates, Europhys. Lett., **5**, 413 (1988).

[22] S. T. Milner, T. A. Witten, and M. E. Cates, Macromolecules, **21**, 2610 (1988).

[23] A. V. Dobrynin, S. P. Obukhov, and M. Rubinshtein, Macromolecules, **32**, 5689 (1999).

[24] J. Feder, J. Theor. Biol., **87**, 237 (1980).

[25] Y. Pomeau, J. Phys. A, **13**, L193 (1980).

[26] R.H. Swendsen, Phys. Rev. A, **24**, 504 (1981).

[27] R.D. Vigil and R.M. Ziff, J. Chem. Phys., **91**, 2599 (1989).

[28] R. Dickman, J.-S. Wang, and I. Jensen, J. Chem. Phys., **94**, 8252 (1991).

[29] P. Viot, G. Tarjus, S.M. Ricci, and J. Talbot, J. Chem. Phys., **97**, 5212 (1992).

[30] J.L. Becklehimer and R.B. Pandey, J. Stat. Phys., **75**, 765 (1994).

[31] J.-S. Wang and R.B. Pandey, Phys. Rev. Lett., **77**, 1773 (1996).

[32] D. Stauffer and A. Aharony, *Introduction to Percolation Theory*, second edition (Taylor & Francis, 1994).

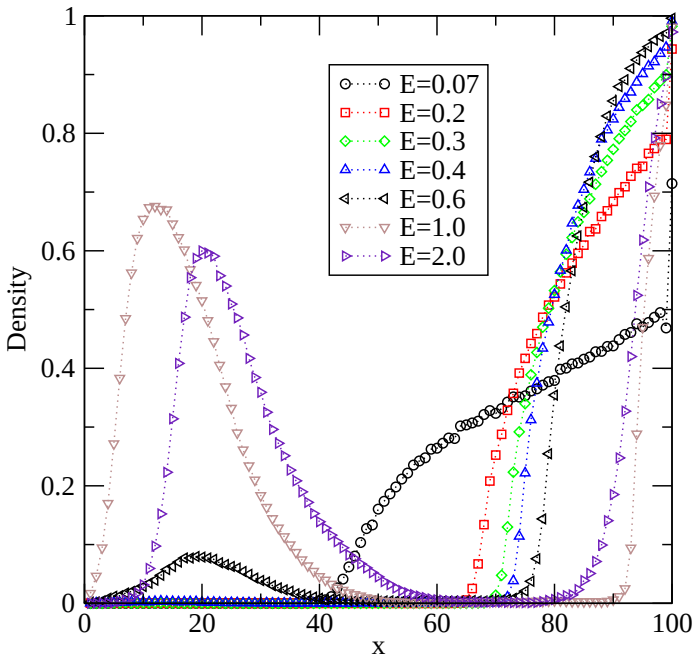

Fig. 1. Density profiles using kink-jump (K) segmental dynamics at various fields with $L_c = 39, T = 1$. Ten to twenty independent samples were used.

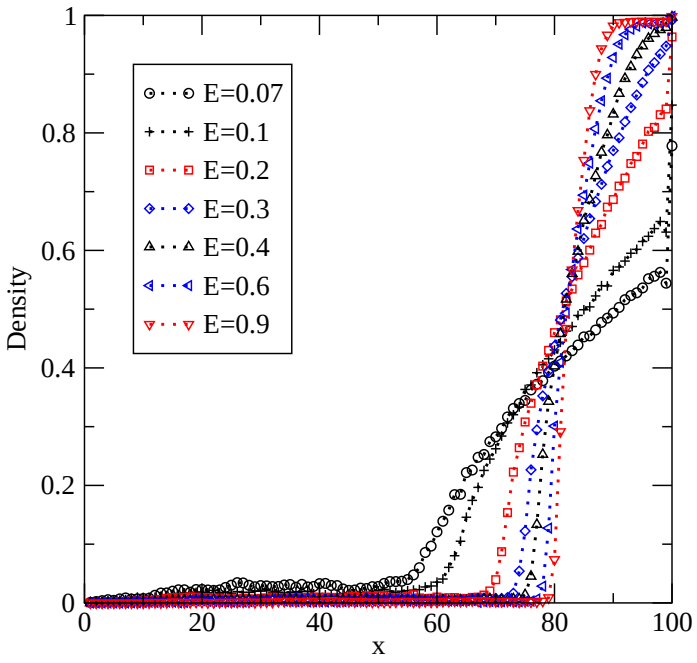

Fig. 2. Density profiles with a combination of kink-jump and crankshaft (KC) segmental dynamics.

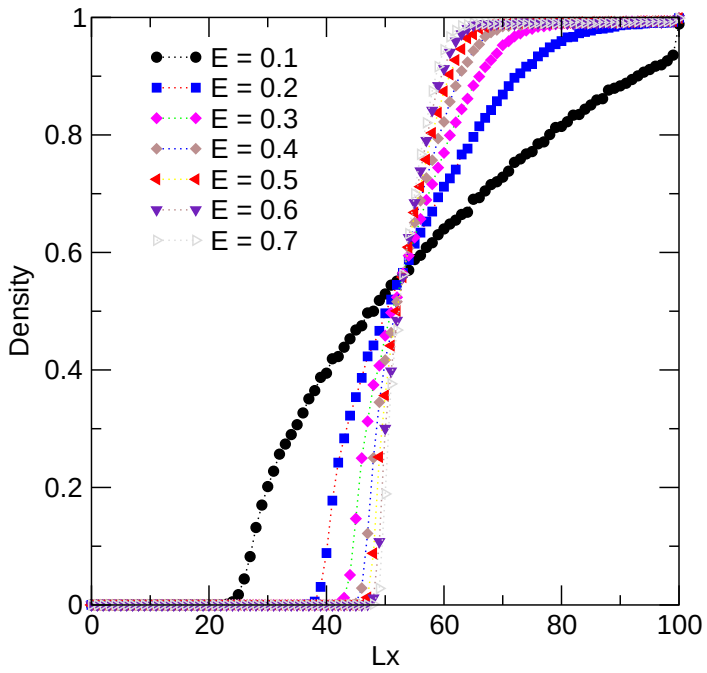

Fig. 3. Density profiles with a combination of kink-jump, crankshaft, and reptation (KCR) segmental dynamics for $L_c = 50$.

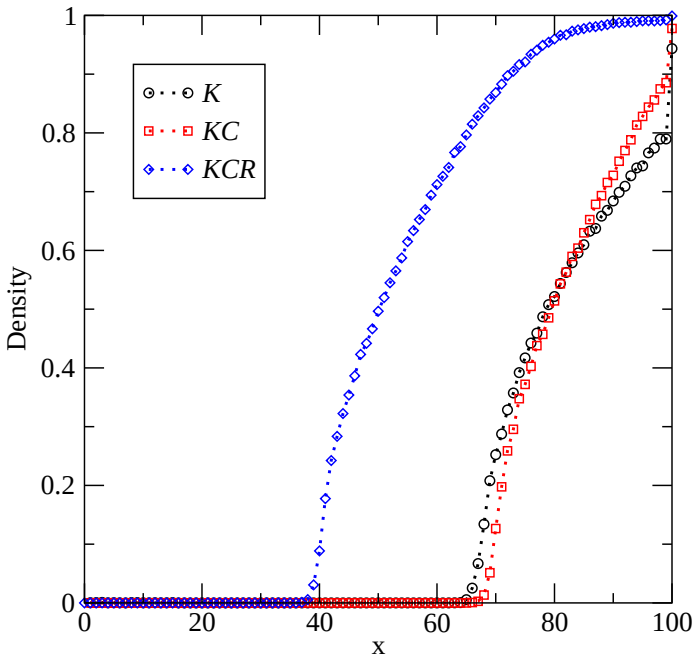

Fig. 4. Density profiles at $T = 1$, $E = 0.2$ with different combinations of segmental dynamics, K, KC with $L_c = 39$, and KCR with $L_c = 50$.

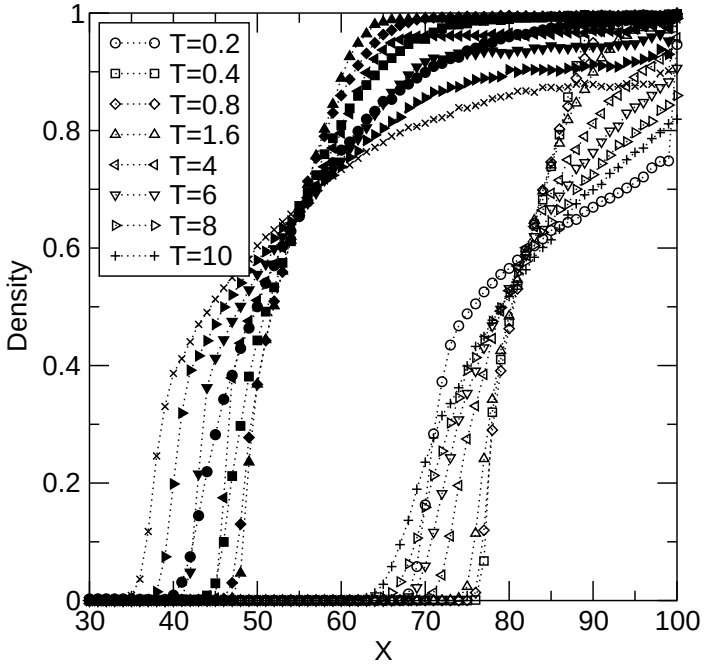

Fig. 5. Density profiles with KC ($L_c = 39$) and KCR ($L_c = 50$) segmental dynamics at various temperatures with $E = 0.5$. Averages were taken over 10 independent simulation runs.

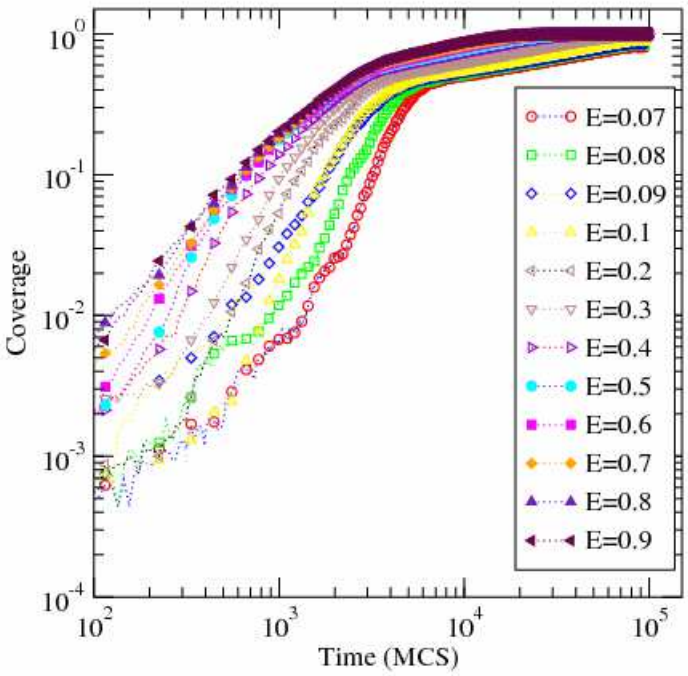

Fig. 6. Growth of coverage with KC segmental dynamics at various fields. Averages were taken over 10 independent simulation runs.

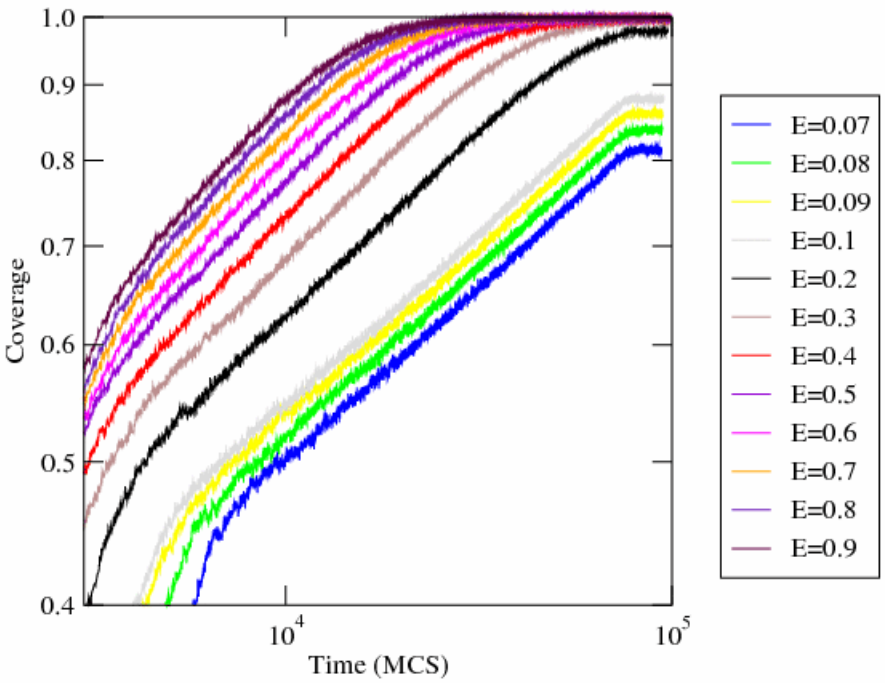

Fig. 7. Same as Fig. 6 in a pre-saturation regions.

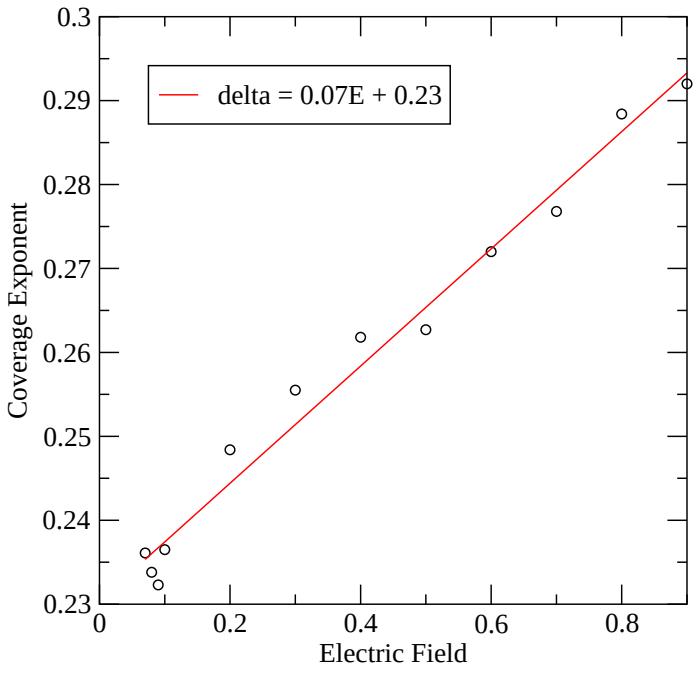

Fig. 8. Variation of pre-saturation growth exponent (Fig. 7) with the field.

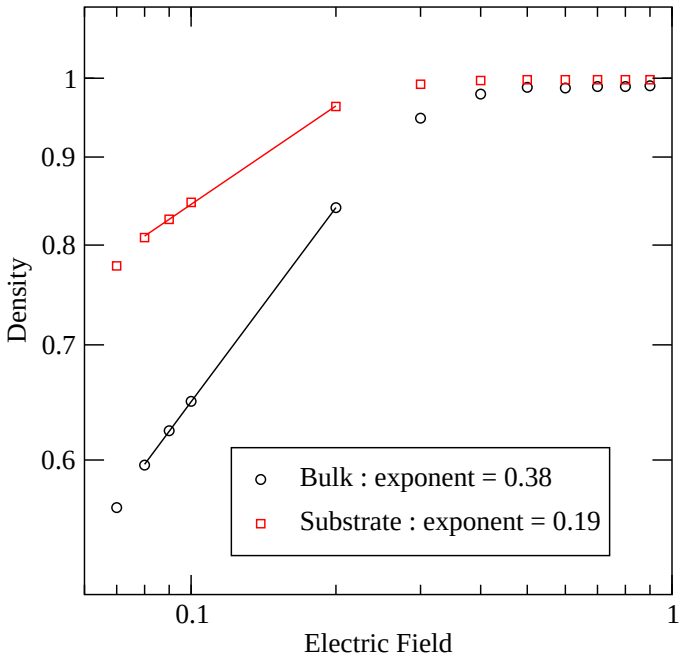

Fig. 9. Variation of the relaxed bulk and substrate density with the field at $T = 1$ with KC segmental dynamics $L_c = 39$. Averages were taken over 10 independent runs.

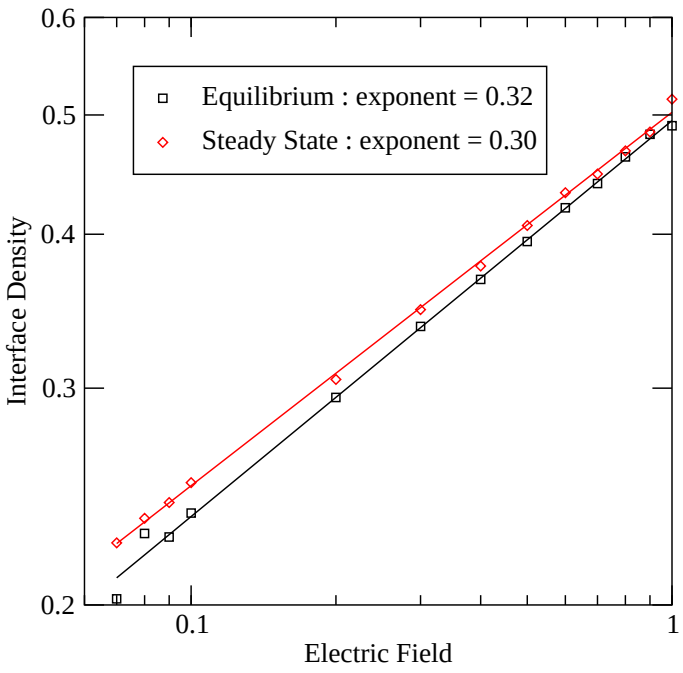

Fig. 10. Variation of the relaxed polymer density (d_f) at the interface (i.e., the front of the bulk) with the field. Results are averaged over 10 independent runs.

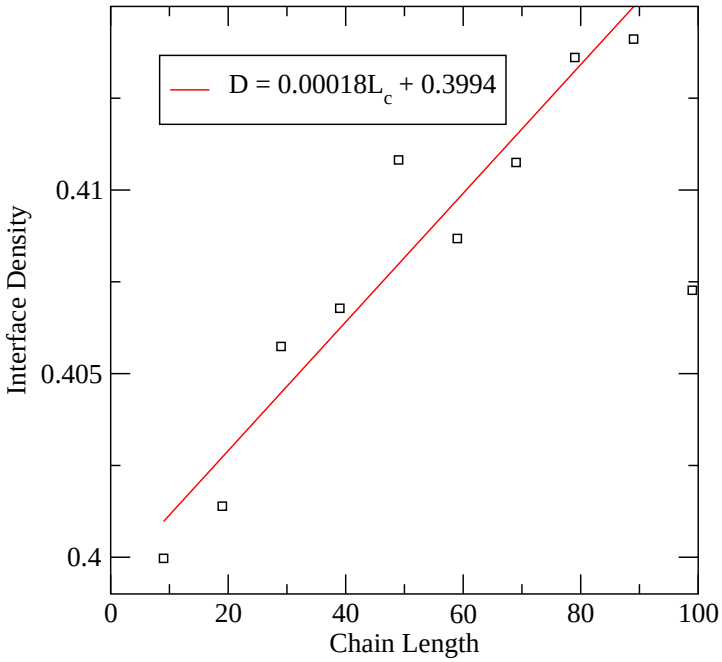

Fig. 11. Variation of the relaxed polymer density at the interface (d_f) with the chain length using $T = 1, E = 0.5$, and 10 independent runs.

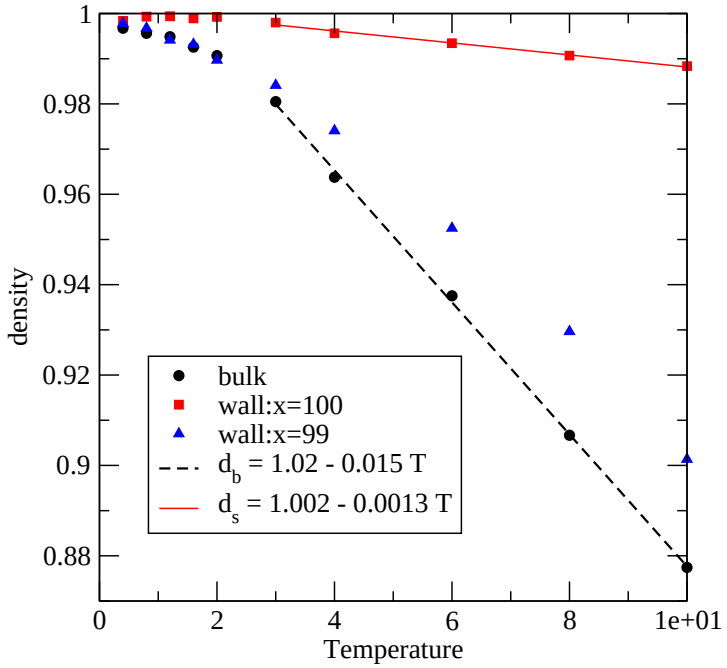

Fig. 12. Variation of the relaxed bulk density (d_b), substrate density (d_s), and polymer density adjacent to substrate (d_{as}) with temperature at $E = 0.5$ with KCR segmental dynamics ($L_c = 39$).

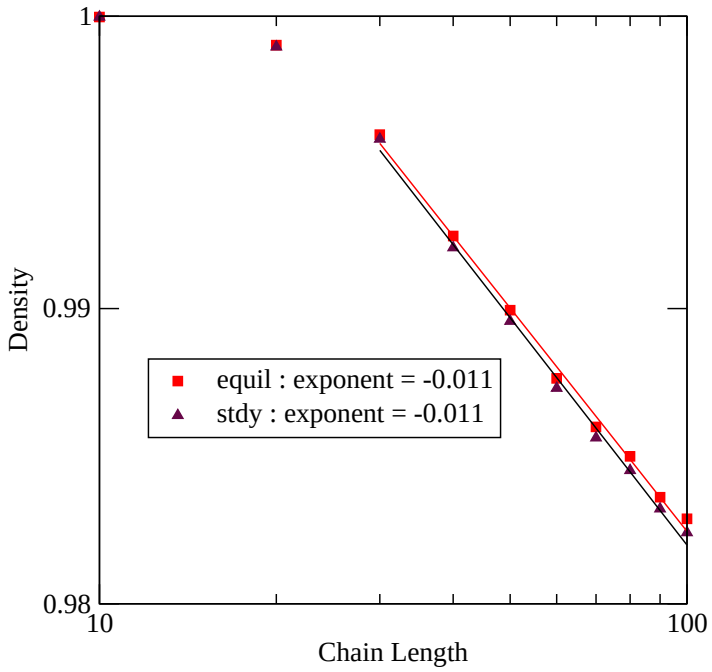

Fig. 13. Bulk density versus chain length with KCR segmental dynamics at $E = 1.0$, $T = 1.0$.

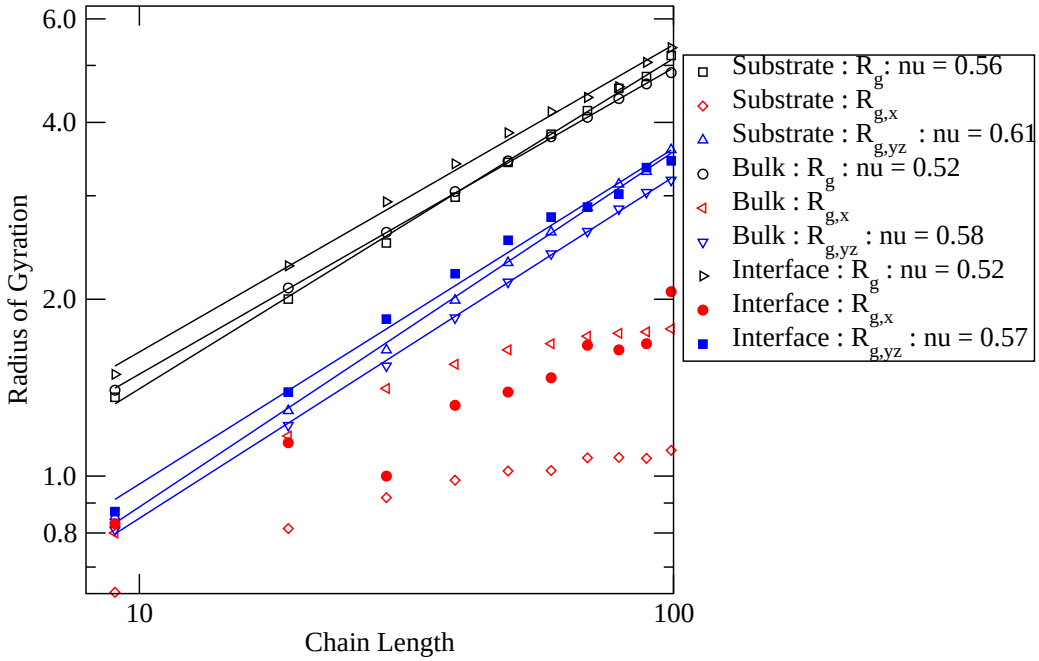

Fig. 14. Variation of the radius of gyration of the polymer chains R_g and its longitudinal (x) and transverse (yz) components with the molecular weight at the substrate, bulk, and interface using KC segmental dynamics at $T = 1$, $E = 0.4$.